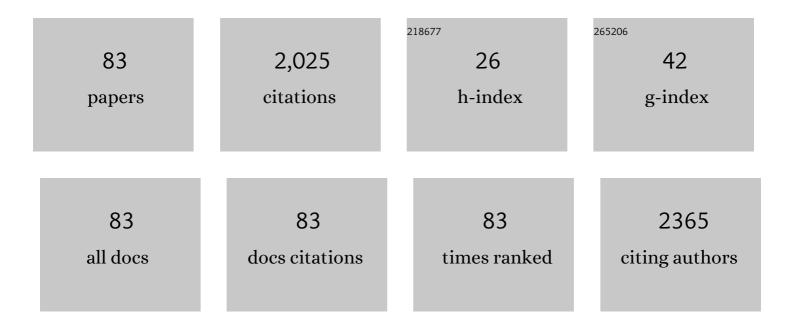
List of Publications by Year in descending order

Source: https://exaly.com/author-pdf/9562275/publications.pdf Version: 2024-02-01



#	Article	IF	CITATIONS
1	Metal(II) Coordination Polymers Derived from Bis-pyridyl-bis-amide Ligands and Carboxylates: Syntheses, Topological Structures, and Photoluminescence Properties. Crystal Growth and Design, 2011, 11, 1662-1674.	3.0	169
2	Metal–organic framework – derived Co ₉ S ₈ @CoS@CoO@C nanoparticles as efficient electro- and photo-catalysts for the oxygen evolution reaction. Journal of Materials Chemistry A, 2017, 5, 10495-10509.	10.3	103
3	Epitaxial grown self-supporting NiSe/Ni3S2/Ni12P5 vertical nanofiber arrays on Ni foam for high performance supercapacitor: Matched exposed facets and re-distribution of electron density. Nano Energy, 2019, 55, 65-81.	16.0	99
4	Novel metal(<scp>ii</scp>) coordination polymers based on N,N′-bis-(4-pyridyl)phthalamide as supercapacitor electrode materials in an aqueous electrolyte. Dalton Transactions, 2013, 42, 1603-1611.	3.3	92
5	Metal–organic frameworks based on naphthalene-1,5-diyldioxy-di-acetate: structures, topologies, photoluminescence and photocatalytic properties. CrystEngComm, 2012, 14, 3727.	2.6	89
6	Calcination/phosphorization of dual Ni/Co-MOF into NiCoP/C nanohybrid with enhanced electrochemical property for high energy density asymmetric supercapacitor. Electrochimica Acta, 2019, 320, 134582.	5.2	78
7	Octamolybdate-Based Metal–Organic Framework with Unsaturated Coordinated Metal Center As Electrocatalyst for Generating Hydrogen from Water. Inorganic Chemistry, 2013, 52, 777-784.	4.0	74
8	Synthesis, Characterization and Activity against <i>Staphylococcus</i> of Metal(II)â€Gatifloxacin Complexes. Chinese Journal of Chemistry, 2007, 25, 1809-1814.	4.9	69
9	Interpenetrated metal–organic frameworks of self-catenated four-connected mok nets. Chemical Communications, 2011, 47, 5982.	4.1	66
10	One-step synthesis of MnS/MoS ₂ /C through the calcination and sulfurization of a bi-metal–organic framework for a high-performance supercapacitor and its photocurrent investigation. Dalton Transactions, 2018, 47, 5390-5405.	3.3	64
11	Metal(II)-Induced Coordination Polymer Based on 4-(5-(Pyridin-4-yl)-4H-1,2,4-triazol-3-yl)benzoate as an Electrocatalyst for Water Splitting. Crystal Growth and Design, 2014, 14, 649-657.	3.0	58
12	(Co, Mn)-Doped NiSe ₂ -diethylenetriamine (dien) nanosheets and (Co, Mn, Sn)-doped NiSe ₂ nanowires for high performance supercapacitors: compositional/morphological evolution and (Co, Mn)-induced electron transfer. Nanoscale, 2019, 11, 16810-16827.	5.6	56
13	MOF-derived Cl/O-doped C/CoO and C nanoparticles for high performance supercapacitor. Applied Surface Science, 2018, 448, 50-63.	6.1	43
14	Low-temperature synthesis of NiS/MoS2/C nanowires/nanoflakes as electrocatalyst for hydrogen evolution reaction in alkaline medium via calcining/sulfurizing metal-organic frameworks. Electrochimica Acta, 2018, 274, 74-83.	5.2	40
15	Metal(ii) complexes based on 1,4-bis(3-pyridylaminomethyl)benzene: structures, photoluminescence and photocatalytic properties. Dalton Transactions, 2013, 42, 13241.	3.3	37
16	Ni-Doped Cobalt Phosphite, Co ₁₁ (HPO ₃) ₈ (OH) ₆ , with Different Morphologies Grown on Ni Foam Hydro(solvo)thermally for High-Performance Supercapacitor. ACS Applied Materials & Interfaces, 2018, 10, 31340-31354.	8.0	37
17	Two Co ^{II} Metal–Organic Frameworks Based on a Multicarboxylate Ligand as Electrocatalysts for Water Splitting. ChemPlusChem, 2014, 79, 266-277.	2.8	35
18	Low temperature synthesis of sponge-like NiV2O6/C composite by calcining Ni-V-based coordination polymer for supercapacitor application. Journal of Electroanalytical Chemistry, 2018, 823, 80-91.	3.8	35

#	Article	IF	CITATIONS
19	Metal–organic frameworks based on 1,3,5-triazine-2,4,6-triyltrithio-triacetate: structures, topologies, photoluminescence and photocatalytic properties. Dalton Transactions, 2013, 42, 7196.	3.3	34
20	Metal–organic frameworks based on rigid ligands as separator membranes in supercapacitor. Dalton Transactions, 2015, 44, 5407-5416.	3.3	34
21	Two novel Co(ii) coordination polymers based on 1,4-bis(3-pyridylaminomethyl)benzene as electrocatalysts for oxygen evolution from water. Dalton Transactions, 2013, 42, 12252.	3.3	32
22	Aluminium vanadate with unsaturated coordinated V centers and oxygen vacancies: surface migration and partial phase transformation mechanism in high performance zinc-ion batteries. Journal of Materials Chemistry A, 2022, 10, 912-927.	10.3	32
23	Reversible color changes of metal(ii)-N1,N3-di(pyridin-4-yl)isophthalamide complexes via desolvation and solvation. Dalton Transactions, 2010, 39, 9923.	3.3	30
24	One-step mild synthesis of Mn-based spinel MnIICrIII2O4/MnIIMnIII2O4/C and Co-based spinel CoCr2O4/C nanoparticles as battery-type electrodes for high-performance supercapacitor application. Electrochimica Acta, 2018, 283, 197-211.	5.2	29
25	Nickel sulfide wrapped by porous cobalt molybdate nanosheet arrays grown on Ni foam for oxygen evolution reaction and supercapacitor. Electrochimica Acta, 2018, 286, 65-76.	5.2	28
26	Cr-doped (Co, Ni)3S4/Co9S8/Ni3S2 nanowires/nanoparticles grown on Ni foam for hybrid supercapacitor. Journal of Alloys and Compounds, 2020, 835, 155254.	5.5	27
27	Chromium vanadate with unsaturated coordination sites for high-performance zinc-ion battery. Chemical Engineering Journal, 2022, 431, 134034.	12.7	27
28	Metal–organic frameworks built from achiral cyclohex-1-ene-1,2-dicarboxylate: syntheses, structures and photoluminescence properties. CrystEngComm, 2012, 14, 5649.	2.6	25
29	Photocurrent-generating properties of bulk and few-layered Cd(<scp>ii</scp>) coordination polymers based on a rigid dicarboxylate ligand. Dalton Transactions, 2016, 45, 4603-4613.	3.3	23
30	Anion-directed assembly: Framework conversion in dimensionality and photoluminescence. Journal of Solid State Chemistry, 2007, 180, 1476-1488.	2.9	22
31	Facile one-pot synthesis of Ni2+-doped (NH4)2V3O8 nanoflakes@Ni foam with visible-light-driven photovoltaic behavior for supercapacitor application. Applied Surface Science, 2018, 439, 33-44.	6.1	22
32	Coordination Polymer-Derived Fe ₃ N Nanoparticles for Efficient Electrocatalytic Oxygen Evolution. Inorganic Chemistry, 2021, 60, 12136-12150.	4.0	21
33	K-doped FeOOH/Fe ₃ O ₄ nanoparticles grown on a stainless steel substrate with superior and increasing specific capacity. Dalton Transactions, 2019, 48, 2491-2504.	3.3	19
34	Synthesis and characterization of metal(II)–fluconazole complexes: Chain-like structure and photoluminescence. Journal of Molecular Structure, 2007, 837, 48-57.	3.6	17
35	Synthesis, structural characterization and anion-sensing studies of metal(<scp>ii</scp>) complexes based on 3,3′,4,4′-oxydiphthalate and N-donor ligands. Dalton Transactions, 2012, 41, 1961-1970.	3.3	17
36	Metal–organic frameworks based on 4-(4-carboxyphenyl)-2,2,4,4-terpyridine: structures, topologies and electrocatalytic behaviors in sodium laurylsulfonate aqueous solution. CrystEngComm, 2014, 16, 9882-9890.	2.6	16

#	Article	IF	CITATIONS
37	Configurations, band structures and photocurrent responses of 4-(4-oxopyridin-1(4H)-yl)phthalic acid and its metal-organic frameworks. Journal of Solid State Chemistry, 2016, 237, 313-322.	2.9	16
38	LaF ₃ Nanosheet-induced Epitaxial Growth: Hollow (Co, Ni) ₂ P/LaF ₃ Nanotube Arrays Built by Porous Heterojunction Walls Grown on Ni Foam as Active Electrocatalyst for Hydrogen Evolution Reaction. Inorganic Chemistry, 2020, 59, 7000-7011.	4.0	16
39	Unsaturated coordination modes of Mn/V in manganese vanadate: Inner capture and surface migration of zinc ions for high performance zinc-ion battery. Journal of Power Sources, 2022, 525, 231134.	7.8	15
40	Metal(ii) complexes based on 4-(2,6-di(pyridin-4-yl)pyridin-4-yl)benzonitrile: structures and electrocatalysis in hydrogen evolution reaction from water. CrystEngComm, 2014, 16, 8492-8499.	2.6	14
41	Ultrafine Co2P anchored on porous CoWO4 nanofiber matrix for hydrogen evolution: Anion-induced compositional/morphological transformation and interfacial electron transfer. Electrochimica Acta, 2019, 328, 135123.	5.2	14
42	Co-Incorporated NiV ₂ O ₆ /Ni(HCO ₃) ₂ nanoflake arrays grown on nickel foam as a high-performance supercapacitor electrode. Dalton Transactions, 2019, 48, 5315-5326.	3.3	14
43	Photocurrent Response of Two ÂMetal(II) Complexes Based on Rigid Ligands. European Journal of Inorganic Chemistry, 2016, 2016, 322-329.	2.0	13
44	A homochiral network constructed by supramolecular packing of 2D chiral bilayer: synthesis, structure and property of metal(ii) complex based on achiral 3,3′,4,4′-oxydiphthalate and coligand. CrystEngComm, 2012, 14, 5862.	2.6	12
45	Facile one-pot synthesis of 2D vanadium-doped NiCl(OH) nanoplates assembled by 3D nanosheet arrays on Ni foam for supercapacitor application. Applied Surface Science, 2019, 478, 75-86.	6.1	12
46	Metal(ii) complexes synthesized based on quinoline-2,3-dicarboxylate as electrocatalysts for the degradation of methyl orange. Dalton Transactions, 2014, 43, 8454-8460.	3.3	11
47	Mg(ii)-induced second-harmonic generation based on bis-monodentate coordination mode of thiobarbiturate. Dalton Transactions, 2013, 42, 6489.	3.3	10
48	A polyoxometalate-based complex with visible-light photochromism as the electrocatalyst for generating hydrogen from water. Dalton Transactions, 2014, 43, 16928-16936.	3.3	10
49	Controllable synthesis of Mo O linkage enhanced CoP ultrathin nanosheet arrays for efficient overall water splitting. Applied Surface Science, 2019, 493, 852-861.	6.1	10
50	Enhanced photocurrent response on a CdTe incorporated coordination polymer based on 3-(3-(1H-imidazol-1-yl)phenyl)-5-(4-(1H-imidazol-1-yl)phenyl)-1-methyl-1H-1,2,4-triazole. RSC Advances, 2016, 6, 73869-73878.	3.6	9
51	The photocurrent response in the perovskite device based on coordination polymers: structure, topology, band gap and matched energy levels. Dalton Transactions, 2017, 46, 7866-7877.	3.3	9
52	F or V-induced activation of (Co, Ni)2P during electrocatalysis for efficient hydrogen evolution reaction. CrystEngComm, 2019, 21, 6080-6092.	2.6	9
53	Iron Coordination Polymer, Fe(oxalate)(H ₂ O) ₂ Nanorods Grown on Nickel Foam via One-Step Electrodeposition as an Efficient Electrocatalyst for Oxygen Evolution Reaction. Inorganic Chemistry, 2021, 60, 5140-5152.	4.0	9
54	Organic molecules induced crystal transformation from a two dimensional coordination polymer to chain-like structures. CrystEngComm, 2012, 14, 663-669.	2.6	8

#	Article	IF	CITATIONS
55	Metal–organic frameworks built from achiral 3-(5-(pyridin-4-yl)-4H-1,2,4-triazol-3-yl)benzoic acid: syntheses and structures of metal(<scp>ii</scp>) complexes. Dalton Transactions, 2014, 43, 145-151.	3.3	8
56	Cu(<scp>i</scp>) complex based on 6H-indolo[2,3-b]quinoxaline: structure and electrocatalytic properties for hydrogen evolution reaction from water. RSC Advances, 2015, 5, 34058-34064.	3.6	8
57	Two novel Pb(II) coordination polymers (CPs) based on 4-(4-oxopyridin-1(4H)-yl) and 3-(4-oxopyridin-1(4H)-yl) phthalic acid: Band gaps, structures, and their photoelectrocatalytic properties in CO2-saturated system. Journal of Solid State Chemistry, 2018, 261, 43-52.	2.9	8
58	Synthesis, Characterization and Properties of Two Novel Complexes Based on 2-Aminopyridine and Polyoxometalatesâ€. Chinese Journal of Chemistry, 2006, 24, 1148-1153.	4.9	7
59	Three in situ-synthesized novel inorganic–organic hybrid materials based on metal (M = Bi, Pb) iodide and organoamine using one-pot reactions: structures, band gaps and optoelectronic properties. New Journal of Chemistry, 2018, 42, 699-707.	2.8	7
60	Coordination polymer-derived Al ³⁺ -doped V ₂ O ₃ /C with rich oxygen vacancies for an advanced aqueous zinc-ion battery with ultrahigh rate capability. Sustainable Energy and Fuels, 2022, 6, 2020-2037.	4.9	7
61	A Facile Electrosynthesis of Terephthalate (tp)â€Based Metalâ€Organic Framework, Ni 3 (OH) 2 (H 2 O) 2 (tp) 2 with Superior Catalytic Activity for Hydrogen Evolution Reaction. European Journal of Inorganic Chemistry, 2020, 2020, 4215-4224.	2.0	6
62	MOFâ€Derived MnV ₂ O ₄ /C Microparticles with Graphene Coating Anchored on Graphite Sheets: Oxygen Defect Engaged High Performance Aqueous Zincâ€Ion Battery. Advanced Materials Interfaces, 2022, 9, .	3.7	6
63	Electrochemical performance of antimony/chlorine-incorporated nickel foam. CrystEngComm, 2019, 21, 7424-7436.	2.6	5
64	Metal(II) Complexes Based on Imidazo[4, 5â€f]â€1, 10â€phenanthroline and Bridging Dicarboxylato Ligands: Synthesis, Characterization and Photoluminescence. Zeitschrift Fur Anorganische Und Allgemeine Chemie, 2012, 638, 473-481.	1.2	4
65	Band Caps and Photocurrent Responses of Bulk and Thinâ€Film Coordination Polymers Based on 3,6â€Di(1 <i>H</i> â€imidazolâ€1â€yl)â€9 <i>H</i> â€carbazole. European Journal of Inorganic Chemistry, 2016, 20 4928-4936.	0269	4
66	Coordination polymer based perovskite device: matched energy levels and photocurrent enhancement in the absence or presence of methanol. CrystEngComm, 2017, 19, 7021-7030.	2.6	4
67	Matched Facetâ€Induced Microflowerâ€Like Li, Niâ€Codoped Zn 3 V 3 O 8 /V 2 O 3 Nanoplate Assemblies Grown on Bambooâ€Like Carbon Nanotube for High Energy Density Lithiumâ€Ion Capacitors. Energy Technology, 2020, , 2000701.	3.8	4
68	P-Functionalized and O-deficient TiO _n /VO _m nanoparticles grown on Ni foam as an electrode for supercapacitors: epitaxial grown heterojunction and visible-light-driven photoresponse. Dalton Transactions, 2020, 49, 4476-4490.	3.3	4
69	Fe-Triazole coordination compound-derived Fe ₂ O ₃ nanoparticles anchored on Fe-MOF/N-doped carbon nanosheets for efficient electrocatalytic oxygen evolution reaction. Dalton Transactions, 2021, 50, 16829-16841.	3.3	4
70	Structural Oxygen Vacancies and Crystalline Defects in Iron Vanadate with Multiple Redox Centers Boosting Surface Migration for Highâ€Performance Zincâ€Ion Battery. Advanced Materials Interfaces, 2022, 9, .	3.7	4
71	Metal(<scp>ii</scp>) complex based on 5-[4-(1H-imidazol-1-yl)phenyl]-2H-tetrazole: the effect of the ligand on the electrodes in a lead-acid battery. CrystEngComm, 2015, 17, 1056-1064.	2.6	3
72	Two polymolybdate-based complexes and their graphene composites with visible-light photo-responses. RSC Advances, 2016, 6, 97890-97898.	3.6	3

#	Article	IF	CITATIONS
73	Band gaps and photocurrent responses of two novel alkaline earth metal(II) complexes based on 4,5-di(4′-carboxylphenyl)benzene. Journal of Solid State Chemistry, 2017, 245, 74-81.	2.9	3
74	Coordination compound-derived Al-doped Fe3O4/C as an efficient electrocatalyst for oxygen evolution reaction. Journal of Solid State Chemistry, 2022, 310, 123049.	2.9	3
75	FLOW SENSING CHARACTERISTICS OF THIN FILM BASED ON MULTI-WALL CARBON NANOTUBES. International Journal of Modern Physics B, 2007, 21, 3473-3476.	2.0	2
76	An acid-stable Zn(ii) complex: electrodeposition in sulfuric acid and the effect on the zinc–lead dioxide battery. Dalton Transactions, 2014, 43, 17129-17135.	3.3	2
77	Metal Complexes Based on 2â€[5â€(3,5â€Dibromophenyl)â€2 <i>H</i> â€1,2,4â€triazolâ€3â€yl]pyridine and Thei Composites with CH ₃ NH ₃ Pbl ₃ : Structures, Band Gaps, and Enhanced Optoelectronic Properties. European Journal of Inorganic Chemistry, 2017, 2017, 1256-1265.	r 2.0	2
78	Na0.11WO3 nanoflake arrays grown on Ni foam for high-performance supercapacitor. Journal of Solid State Electrochemistry, 2019, 23, 2141-2152.	2.5	2
79	Coordination compound-derived La-doped FeS ₂ /N-doped carbon (NC) as an efficient electrocatalyst for oxygen evolution reaction. CrystEngComm, 0, , .	2.6	2
80	Syntheses, Crystal Structures, and Photoluminescence Properties of Three Bisâ€acylamide Compounds. Zeitschrift Fur Anorganische Und Allgemeine Chemie, 2012, 638, 438-442.	1.2	1
81	Coordination polymer-based supercapacitors with matched energy levels: enhanced capacity under visible light illumination in the presence of methanol. Dalton Transactions, 2018, 47, 11146-11157.	3.3	1
82	Synthesis, Structure, and Band Gap of a Novel Inorganic–Organic Hybrid Material Based on Antimony Halide and Organoamine. Crystallography Reports, 2018, 63, 433-437.	0.6	1
83	Coordination compound-derived Fe4N/Fe3N/Fe/CNT for efficient electrocatalytic oxygen evolution: a facile one-step synthesis in absence of extra nitrogen source. Nanotechnology, 0, , .	2.6	Ο